

The First Sources of Light

Volker Bromm* and Abraham Loeb*†

**Astronomy Department, Harvard University, 60 Garden St., Cambridge, MA 02138*

†*Institute for Advanced Study, Princeton, NJ 08540; Guggenheim Fellow*

Abstract. We review recent theoretical results on the formation of the first stars and quasars in the universe, and emphasize related open questions. In particular, we list important differences between the star formation process at high redshifts and in the present-day universe. We address the importance of heavy elements in bringing about the transition from an early star formation mode dominated by massive stars, to the familiar mode dominated by low mass stars, at later times. We show how gamma-ray bursts can be utilized to probe the first epoch of star formation. Finally, we discuss how the first supermassive black holes could have formed through the direct collapse of primordial gas clouds.

INTRODUCTION

The first sources of light ionized [1, 2] and metal-enriched [3] the intergalactic medium (IGM) and consequently had important effects on subsequent galaxy formation [4] and on the large-scale polarization anisotropies of the cosmic microwave background [5]. *When did the cosmic dark ages end?* In the context of popular cold dark matter (CDM) models of hierarchical structure formation, the first stars are predicted to have formed in dark matter halos of mass $\sim 10^6 M_\odot$ that collapsed at redshifts $z \simeq 20 - 30$ [4, 6]. The first quasars, on the other hand, are likely to have formed in more massive host systems, at redshifts $z \geq 10$ [7], and certainly before $z \sim 6.4$, the redshift of the most distant quasar known [8].

Results from recent numerical simulations of the collapse and fragmentation of primordial clouds suggest that the first stars were predominantly very massive, with typical masses $M_* \geq 100 M_\odot$ [9, 10, 11, 12]. Despite the progress already made, many important questions remain unanswered; the purpose of this brief review is to discuss these open questions and to put them in perspective. An example for an open question is: *How does the primordial initial mass function (IMF) look like?* Having constrained the characteristic mass scale, still leaves undetermined the overall range of stellar masses and the power-law slope which is likely to be a function of mass. In addition, it is presently unknown whether binaries or, more generally, clusters of zero-metallicity stars, can form. Evidently, the observational signature as well as the fate of the first stars depend sensitively on whether primordial star formation is predominantly clustered or isolated. This in turn is affected by the nature of the feedback that the first stars exert on their surroundings. The first stars are expected to produce copious amounts of UV photons and to possibly explode as energetic hypernovae. *How effective will their negative feedback be in suppressing star formation in neighboring high-density clumps?*

Predicting the properties of the first stars is important for the design of upcoming

instruments, such as the *James Webb Space Telescope* (JWST)¹, or the next generation of large (> 10 m) ground-based telescopes. The hope is that over the upcoming decade, it will become possible to confront current theoretical predictions about the properties of the first sources of light with direct observational data. The increasing volume of new data on high redshift galaxies and quasars from existing ground-based telescopes, signals the emergence of this new frontier in cosmology.

STAR FORMATION THEN AND NOW

Currently, we do not have direct observational constraints on how the first stars, the so-called Population III stars, formed at the end of the cosmic dark ages. It is, therefore, instructive to briefly summarize what we have learned about star formation in the present-day universe, where theoretical reasoning is guided by a wealth of observational data (see [13] for a recent review).

Population I stars form out of cold, dense molecular gas that is structured in a complex, highly inhomogeneous way. The molecular clouds are supported against gravity by turbulent velocity fields and pervaded on large scales by magnetic fields. Stars tend to form in clusters, ranging from a few hundred up to $\sim 10^6$ stars. It appears likely that the clustered nature of star formation leads to complicated dynamics and tidal interactions that transport angular momentum, thus allowing the collapsing gas to overcome the classical centrifugal barrier [14]. The IMF of Pop I stars is observed to have the approximate Salpeter form (e.g., [15])

$$\frac{dN}{d\log M} \propto M^x, \quad (1)$$

where

$$x \simeq \begin{cases} -1.35 & \text{for } M \geq 0.5M_\odot \\ 0.0 & \text{for } 0.007 \leq M \leq 0.5M_\odot \end{cases}. \quad (2)$$

The lower cutoff in mass corresponds roughly to the opacity limit for fragmentation. This limit reflects the minimum fragment mass, set when the rate at which gravitational energy is released during the collapse exceeds the rate at which the gas can cool (e.g., [16]). The most important feature of the observed IMF is that $\sim 1M_\odot$ is the characteristic mass scale of Pop I star formation, in the sense that most of the mass goes into stars with masses close to this value. In Figure 1, we show the result from a recent hydrodynamical simulation of the collapse and fragmentation of a molecular cloud core [17, 18]. This simulation illustrates the highly dynamic and chaotic nature of the star formation process².

The metal-rich chemistry, magnetohydrodynamics, and radiative transfer involved in present-day star formation is complex, and we still lack a comprehensive theoretical framework that predicts the IMF from first principles. Star formation in the high redshift universe, on the other hand, poses a theoretically more tractable problem due to a

¹ See <http://ngst.gsfc.nasa.gov>.

² See <http://www.ukaff.ac.uk/starcluster> for an animation.

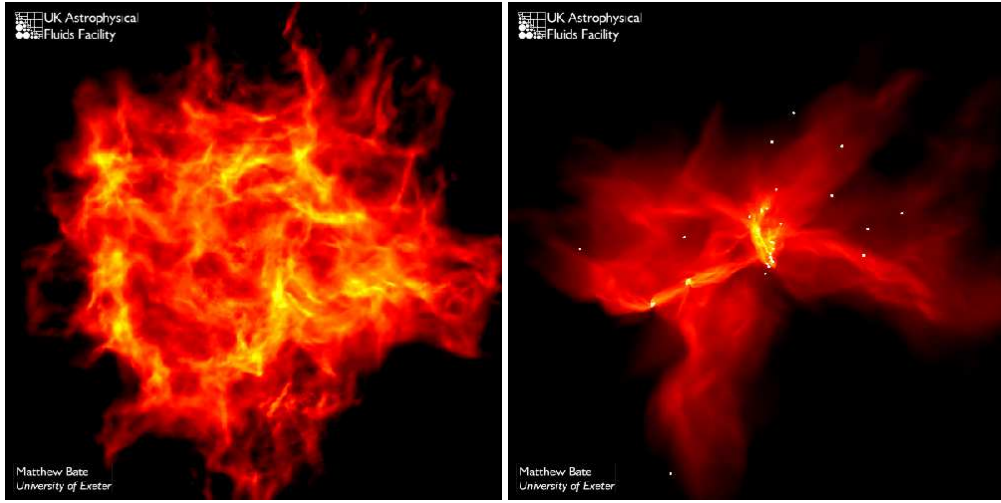


FIGURE 1. A hydrodynamic simulation of the collapse and fragmentation of a turbulent molecular cloud in the present-day universe (from [18]). The cloud has a mass of $50M_{\odot}$. The panels show the column density through the cloud, and span a scale of 0.4 pc across. *Left:* The initial phase of the collapse. The turbulence organizes the gas into a network of filaments, and decays thereafter through shocks. *Right:* A snapshot taken near the end of the simulation, after 1.4 initial free-fall times of 2×10^5 yr. Fragmentation has resulted in ~ 50 stars and brown dwarfs. The star formation efficiency is $\sim 10\%$ on the scale of the overall cloud, but can be much larger in the dense sub-condensations. This result is in good agreement with what is observed in local star-forming regions.

number of simplifying features, such as: (i) the initial absence of heavy metals and therefore of dust; and (ii) the absence of dynamically-significant magnetic fields, in the pristine gas left over from the big bang. The cooling of the primordial gas does then only depend on hydrogen in its atomic and molecular form. Whereas in the present-day interstellar medium, the initial state of the star forming cloud is poorly constrained, the corresponding initial conditions for primordial star formation are simple, given by the popular Λ CDM model of cosmological structure formation. We now turn to a discussion of this theoretically attractive and important problem.

PRIMORDIAL STAR FORMATION

How did the first stars form? A complete answer to this question would entail a theoretical prediction for the Population III IMF, which is rather challenging. Let us start by addressing the simpler problem of estimating the characteristic mass scale of the first stars. As mentioned before, this mass scale is observed to be $\sim 1M_{\odot}$ in the present-day universe. To investigate the collapse and fragmentation of primordial gas, we have carried out numerical simulations, using the smoothed particle hydrodynamics (SPH) method. We have included the chemistry and cooling physics relevant for the evolution of metal-free gas (see [10] for details). Improving on earlier work [9, 10] by initializing our simulation according to the Λ CDM model, we focus here on an isolated overdense region that corresponds to a 3σ —peak: a halo containing a total mass of 10^6M_{\odot} , and

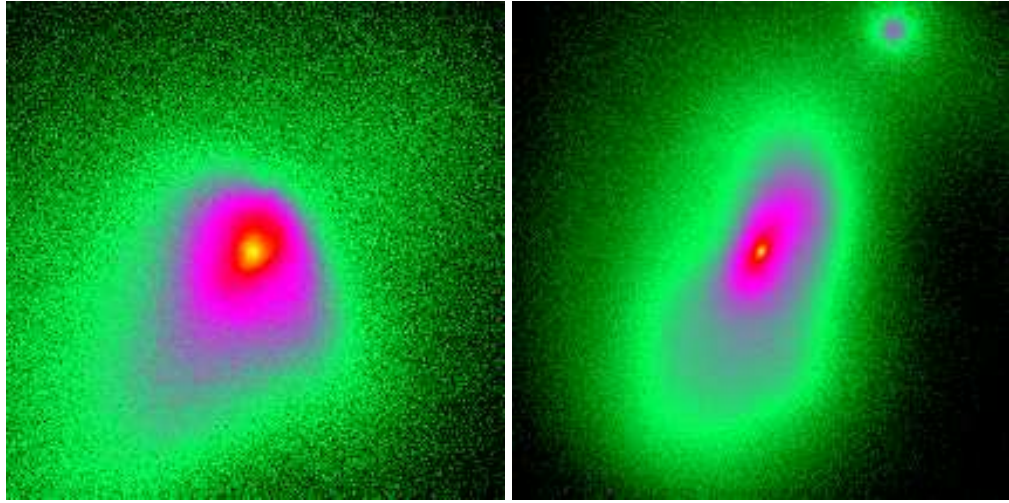


FIGURE 2. Collapse and fragmentation of a primordial cloud. Shown is the projected gas density at a redshift $z \simeq 21.5$, briefly after gravitational runaway collapse has commenced in the center of the cloud. *Left:* The coarse-grained morphology in a box with linear physical size of 23.5 pc. At this time in the unrefined simulation, a high-density clump (sink particle) has formed with an initial mass of $\sim 10^3 M_\odot$. *Right:* The fine-grain morphology in a box with linear physical size of 0.5 pc. The central density peak, vigorously gaining mass by accretion, is accompanied by a secondary clump.

collapsing at a redshift $z_{\text{vir}} \simeq 20$.

In Figure 2 (*left panel*), we show the gas density within the central ~ 25 pc, briefly after the first high-density clump has formed as a result of gravitational runaway collapse. Once the gas has exceeded a threshold density of 10^7 cm^{-3} , a sink particle is inserted into the simulation to replace it. This choice for the density threshold ensures that the local Jeans mass is resolved throughout the simulation. The clump (i.e., sink particle) has an initial mass of $M_{\text{Cl}} \sim 10^3 M_\odot$, and grows subsequently by ongoing accretion of surrounding gas. High-density clumps with such masses result from the chemistry and cooling rate of molecular hydrogen, H_2 , which imprint characteristic values of temperature, $T \sim 200 \text{ K}$, and density, $n \sim 10^4 \text{ cm}^{-3}$, into the metal-free gas (see [10]). Evaluating the Jeans mass for these characteristic values results in $M_J \sim 10^3 M_\odot$, which is close to the initial clump masses found in the simulations.

The high-density clumps are clearly not stars yet. To probe the subsequent fate of a clump, we have re-simulated the evolution of the central clump with sufficient resolution to follow the collapse to higher densities (see [19] for a description of the refinement technique). In Figure 2 (*right panel*), we show the gas density on a scale of 0.5 pc, which is two orders of magnitude smaller than before. Several features are evident in this plot. First, the central clump does not undergo further sub-fragmentation, and is likely to form a single Population III star. Second, a companion clump is visible at a distance of ~ 0.25 pc. If negative feedback from the first-forming star is ignored, this companion clump would undergo runaway collapse on its own approximately ~ 3 Myr later. This timescale is comparable to the lifetime of a very massive star (VMS)[20]. If the second clump was able to survive the intense radiative heating from its neighbor, it could become a star before the first one explodes as a supernova (SN). Whether more

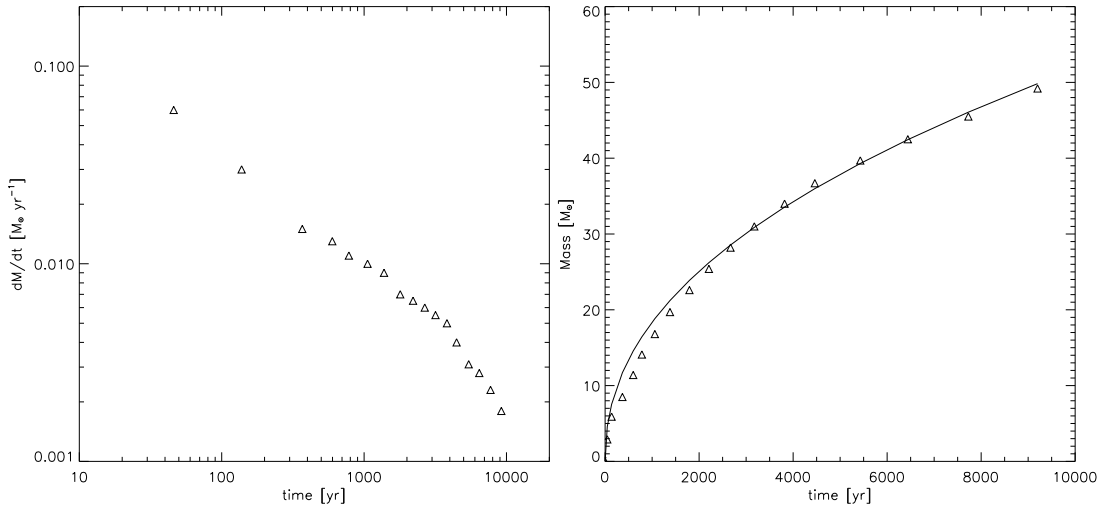


FIGURE 3. Accretion onto a primordial protostar. The morphology of this accretion flow is shown in Fig. 2. *Left:* Accretion rate (in $M_\odot \text{ yr}^{-1}$) vs. time (in yr) since molecular core formation. *Right:* Mass of the central core (in M_\odot) vs. time. *Solid line:* Accretion history approximated as: $M_* \propto t^{0.45}$. Using this analytical approximation, we extrapolate that the protostellar mass has grown to $\sim 150M_\odot$ after $\sim 10^5$ yr, and to $\sim 700M_\odot$ after $\sim 3 \times 10^6$ yr, the total lifetime of a very massive star.

than one star can form in a low-mass halo thus crucially depends on the degree of synchronization of clump formation. Finally, the non-axisymmetric disturbance induced by the companion clump, as well as the angular momentum stored in the orbital motion of the binary system, allow the system to overcome the angular momentum barrier for the collapse of the central clump (see [14]).

The recent discovery of the star HE0107-5240 with a mass of $0.8M_\odot$ and an iron abundance of $[\text{Fe}/\text{H}] = -5.3$ [21] shows that at least some low mass stars could have formed out of extremely low-metallicity gas. Our simulations show that although the majority of clumps are very massive, a few of them, like the secondary clump in Fig. 2, are significantly less massive. Alternatively, low-mass fragments could form in the dense, shock-compressed shells that surround the first hypernovae [22].

How massive were the first stars? Star formation typically proceeds from the ‘inside-out’, through the accretion of gas onto a central hydrostatic core. Whereas the initial mass of the hydrostatic core is very similar for primordial and present-day star formation [23], the accretion process – ultimately responsible for setting the final stellar mass, is expected to be rather different. On dimensional grounds, the accretion rate is simply related to the sound speed cubed over Newton’s constant (or equivalently given by the ratio of the Jeans mass and the free-fall time): $\dot{M}_{\text{acc}} \sim c_s^3/G \propto T^{3/2}$. A simple comparison of the temperatures in present-day star forming regions ($T \sim 10$ K) with those in primordial ones ($T \sim 200 - 300$ K) already indicates a difference in the accretion rate of more than two orders of magnitude.

Our refined simulation enables us to study the three-dimensional accretion flow around the protostar (see also [24, 25, 26]). We now allow the gas to reach densities of 10^{12} cm^{-3} before being incorporated into a central sink particle. At these high densities, three-body reactions [27] have converted the gas into a fully molecular form. In

Figure 3, we show how the molecular core grows in mass over the first $\sim 10^4$ yr after its formation. The accretion rate (*left panel*) is initially very high, $\dot{M}_{\text{acc}} \sim 0.1 M_{\odot} \text{ yr}^{-1}$, and subsequently declines according to a power law, with a possible break at ~ 5000 yr. The mass of the molecular core (*right panel*), taken as an estimator of the proto-stellar mass, grows approximately as: $M_* \sim \int \dot{M}_{\text{acc}} dt \propto t^{0.45}$. A rough upper limit for the final mass of the star is then: $M_*(t = 3 \times 10^6 \text{ yr}) \sim 700 M_{\odot}$. In deriving this upper bound, we have conservatively assumed that accretion cannot go on for longer than the total lifetime of a VMS.

Can a Population III star ever reach this asymptotic mass limit? The answer to this question is not yet known with any certainty, and it depends on whether the accretion from a dust-free envelope is eventually terminated by feedback from the star (e.g., [24, 25, 26, 28]). The standard mechanism by which accretion may be terminated in metal-rich gas, namely radiation pressure on dust grains [29], is evidently not effective for gas with a primordial composition. Recently, it has been speculated that accretion could instead be turned off through the formation of an H II region [28], or through the radiation pressure exerted by trapped Ly α photons [26]. The termination of the accretion process defines the current unsolved frontier in studies of Population III star formation. Current simulations indicate that the first stars were predominantly very massive, and consequently rather different from present-day stellar populations. The crucial question then arises: *How and when did the transition take place from the early formation of massive stars to that of low-mass stars at later times?* We address this problem next.

THE SECOND GENERATION OF STARS

The very first stars, marking the cosmic Renaissance of structure formation, formed under conditions that were much simpler than the highly complex environment in present-day molecular clouds. Subsequently, however, the situation rapidly became more complicated again due to the feedback from the first stars on the IGM. Supernova explosions dispersed the nucleosynthetic products from the first generation of stars into the surrounding gas (e.g., [30, 31, 32]), including also dust grains produced in the explosion itself [33, 34]. Atomic and molecular cooling became much more efficient after the addition of these metals. Moreover, the presence of ionizing cosmic rays, as well as of UV and X-ray background photons, modified the thermal and chemical behavior of the gas in important ways (e.g., [35, 36]).

Early metal enrichment was likely the dominant effect that brought about the transition from Population III to Population II star formation. Recent numerical simulations of collapsing primordial objects with overall masses of $\sim 10^6 M_{\odot}$, have shown that the gas has to be enriched with heavy elements to a minimum level of $Z_{\text{crit}} \simeq 10^{-3.5} Z_{\odot}$, in order to have any effect on the dynamics and fragmentation properties of the system [37, 38]. Normal, low-mass (Population II) stars are hypothesized to only form out of gas with metallicity $Z \geq Z_{\text{crit}}$. Thus, the characteristic mass scale for star formation is expected to be a function of metallicity, with a discontinuity at Z_{crit} where the mass scale changes by \sim two orders of magnitude. The redshift where this transition occurs has important implications for the early growth of cosmic structure, and the resulting observational

signature (e.g., [1, 3, 22, 39]).

Important caveats, however, remain. The determination of the critical metallicity mentioned above [38] implicitly assumes that the gas at temperatures below ~ 8000 K is maintained in ionization equilibrium by cosmic rays, with an ionization rate that is scaled from the Galactic value by the factor Z/Z_{\odot} . The cosmic-ray flux in the early universe might well have not obeyed this simple relation, and it is not clear whether cosmic rays could have successfully ‘activated’ the metals.

GAMMA-RAY BURSTS AS PROBES OF THE FIRST STARS

Gamma-ray bursts (GRBs) are the brightest electromagnetic explosions in the universe, and they should be detectable out to redshifts $z > 10$ [40, 41]. Although the nature of the central engine that powers the relativistic jets is still debated, recent evidence indicates that GRBs trace the formation of massive stars [42, 43, 44, 45, 46]. Since the first stars are predicted to be predominantly very massive, their death might possibly give rise to GRBs at very high redshifts. A detection of the highest-redshift GRBs would probe the earliest epochs of star formation, one massive star at a time. The upcoming *Swift* satellite³, planned for launch in late 2003, is expected to detect about a hundred GRBs per year. The redshifts of high- z GRBs can be easily measured through infrared photometry, based on the Gunn-Peterson trough in their spectra due to Ly α absorption by neutral intergalactic hydrogen along the line of sight. *Which fraction of the detected bursts will originate at redshifts $z \geq 5$?*

To assess the utility of GRBs as probes of the first stars, we have calculated the expected redshift distribution of GRBs [47]. Under the assumption that the GRB rate is simply proportional to the star formation rate, we find that about a quarter of all GRBs detected by *Swift*, will originate from a redshift $z \geq 5$ (see Fig. 4). This estimate is rather uncertain because of the poorly determined GRB luminosity function. We caution that the rate of high-redshift GRBs may be significantly suppressed if the early massive stars fail to launch a relativistic outflow. This is conceivable, as metal-free stars may experience negligible mass loss before exploding as a supernova. They would then retain their massive hydrogen envelope, and any relativistic jet might be quenched before escaping from the star [48].

If high-redshift GRBs exist, the launch of *Swift* later this year will open up an exciting new window into the cosmic dark ages. In difference from quasars or galaxies that fade with increasing redshift, GRB afterglows maintain a roughly constant observed flux at different redshifts for a fixed observed time lag after the γ -ray trigger [41]. The increase in the luminosity distance at higher redshifts is compensated by the fact that a fixed observed time lag corresponds to an intrinsic time shorter by a factor of $(1+z)$ in the source rest-frame, during which the GRB afterglow emission is brighter. This quality makes GRB afterglows the best probes of the metallicity and ionization state of the intervening IGM during the epoch of reionization. In difference from quasars, the UV

³ See <http://swift.gsfc.nasa.gov>.

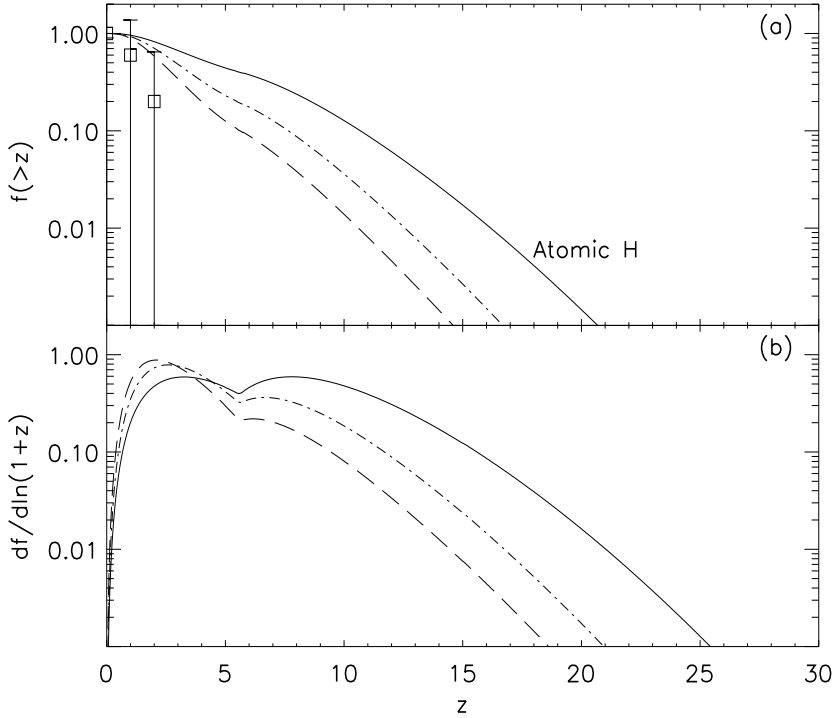


FIGURE 4. Redshift distribution of all GRBs in comparison with measurements in flux-limited surveys (from [47]). (a) Fraction of bursts that originate at a redshift higher than z vs. z . The data points reflect ~ 20 observed redshifts to date. (b) Fraction of bursts per logarithmic interval of $(1+z)$ vs. z . *Solid lines*: All GRBs for star formation in halos massive enough to allow cooling via lines of atomic hydrogen. The calculation assumes that the GRB rate is proportional (with a constant factor) to the star formation rate at all redshifts. *Dot-dashed lines*: Expected distribution for *Swift*. *Long-dashed lines*: Expected distribution for *BATSE*. The curves for the two flux-limited surveys are rather uncertain because of the poorly-determined GRB luminosity function.

emission from GRBs has a negligible effect on the surrounding IGM (since $\sim 10^{51}$ ergs can only ionize $\sim 4 \times 10^4 M_\odot$ of hydrogen). Moreover, the host galaxies of GRBs induce a much weaker perturbation to the Hubble flow in the surrounding IGM, compared to the massive hosts of the brightest quasars [49]. Hence, GRB afterglows offer the ideal probe (much better than quasars or bright galaxies) of the damping wing of the Gunn-Peterson trough [50] that signals the neutral fraction of the IGM as a function of redshift during the epoch of reionization.

THE FIRST QUASARS

Quasars are believed to be powered by the heat generated during the accretion of gas onto supermassive black holes (SMBHs; see e.g., [51]). The existence of SMBHs with

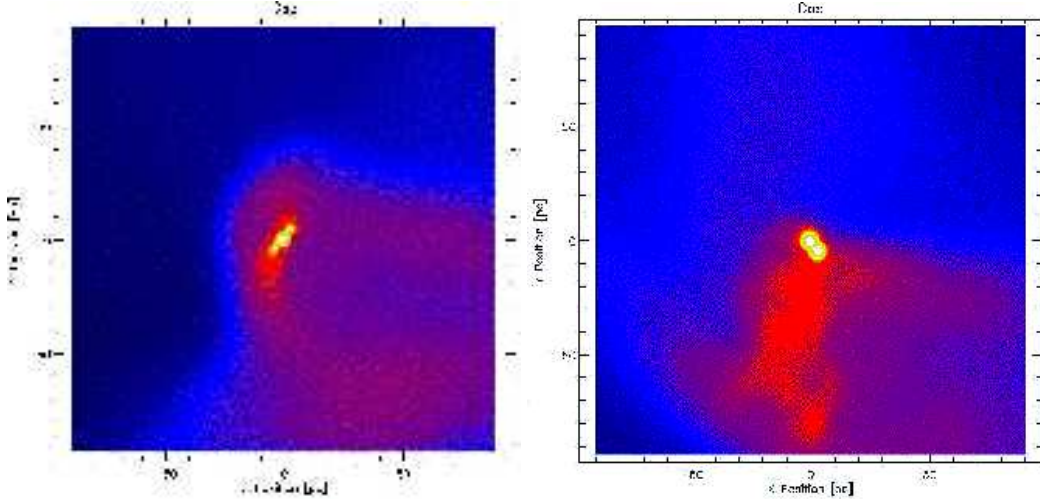


FIGURE 5. Central gas densities in simulations of two dwarf galaxies just above the atomic cooling threshold at $z \sim 10$ with different initial spins and no H_2 molecules (from [19]). Shown is the projection in the $x - y$ plane, and the box size is 200 pc on a side. *Left:* Case with zero initial spin. One compact object has formed in the center with a mass of $2.7 \times 10^6 M_\odot$ and a radius of ≤ 1 pc. *Right:* Case with an initial spin of $\lambda = 0.05$. Here, two compact objects have formed with masses of $2.2 \times 10^6 M_\odot$ and $3.1 \times 10^6 M_\odot$, respectively, and radii ≤ 1 pc.

inferred masses of $\geq 10^9 M_\odot$, less than a billion years after the big bang, as implied by the recent discovery of quasars at redshifts $z \geq 6$ [8, 52, 53, 54], provides important constraints on the SMBH formation scenario [7]. The brightest quasars at $z \geq 6$ are most likely hosted by rare galaxies, more massive than $\sim 10^{12} M_\odot$ [49], that end up today as the most massive elliptical galaxies [55]. *Can the seeds of SMBHs form through the direct collapse of primordial gas clouds at high redshifts?* Previous work [56] has shown that without a pre-existing central point mass, this is rendered difficult by the negative feedback resulting from star formation in the collapsing cloud. The input of kinetic energy due to supernova explosions prevents the gas from assembling in the center of the dark matter potential well, thus precluding the direct formation of a SMBH. If, however, star formation was suppressed in a cloud that could still undergo overall collapse, such an adverse feedback would not occur.

We have carried out SPH simulations [19] of isolated 2σ -peaks with total masses of $10^8 M_\odot$ that collapse at $z_{\text{vir}} \sim 10$. The virial temperature of these dwarf galaxies exceeds $\sim 10^4 \text{ K}$, so as to allow collapse of their gas through cooling by atomic hydrogen transitions [57]. Since structure formation proceeds in a bottom-up fashion, such a system would encompass lower-mass halos that would have collapsed earlier on. These subsystems have virial temperatures below 10^4 K , and consequently rely on the presence of H_2 for their cooling. Molecular hydrogen, however, is fragile and readily destroyed by photons in the Lyman-Werner bands with energies (11.2 – 13.6 eV) just below the Lyman limit [58]. These photons are able to penetrate a predominantly neutral IGM.

We first consider the limiting case in which H_2 destruction is complete. Depending on the initial spin, which is a measure of the degree of rotational support in the cloud, we find that either one (for zero initial spin) or two compact objects form with masses

in excess of $10^6 M_\odot$ and radii < 1 pc (see Fig. 5). In the case of nonzero spin a binary system of clumps has formed with a separation of ~ 10 pc. Such a system of two compact objects is expected to efficiently radiate gravitational waves that could be detectable with the planned *Laser Interferometer Space Antenna*⁴ (LISA)[59].

What is the further fate of the central object? Once the gas has collapsed to densities above $\sim 10^{17}$ cm⁻³ and radii $< 10^{16}$ cm, Thomson scattering traps the photons, and the cooling time consequently becomes much larger than both the free-fall and viscous timescales (see [19] for details). The gas is therefore likely to settle into a radiation-pressure supported configuration resembling a rotating supermassive star. Recent fully-relativistic calculations of the evolution of such stars predict that they would inevitably collapse to a massive black hole [60]. Under a wide range of initial conditions, a substantial fraction ($\sim 90\%$) of the mass of the supermassive star is expected to end up in the black hole.

Is such a complete destruction of H₂ possible? When we include an external background of soft UV radiation in our simulation, we find that a flux level comparable to what is expected close to the end of the reionization epoch is sufficient to suppress H₂ molecule formation. This is the case even when the effect of self-shielding is taken into account. The effective suppression of H₂ formation crucially depends on the presence of a stellar-like radiation background. It is therefore likely that stars existed before the first quasars could have formed.

ACKNOWLEDGMENTS

VB thanks the Institute for Advanced Study for its hospitality during part of the work on this review, and expresses his gratitude to Paolo Coppi and Richard Larson for the many discussions on the first stars. AL acknowledges support from the Institute for Advanced Study at Princeton, the John Simon Guggenheim Memorial Fellowship, and NSF grants AST-0071019, AST-0204514.

REFERENCES

1. Wyithe, J. S. B., & Loeb, A. 2003a, ApJ, in press (astro-ph/0209056)
2. Cen, R. 2003, ApJ, submitted (astro-ph/0210473)
3. Furlanetto, S. R., & Loeb, A. 2003, ApJ, in press (astro-ph/0211496)
4. Barkana, R., & Loeb, A. 2001, Physics Reports, 349, 125
5. Kaplinghat, M., Chu, M., Haiman, Z., Holder, G., Knox, L., & Skordis, C. 2002, ApJ, submitted (astro-ph/0207591)
6. Yoshida, N., Abel, T., Hernquist, L., & Sugiyama, N. 2003, ApJ, submitted
7. Haiman, Z., & Loeb, A. 2001, ApJ, 552, 459
8. Fan, X., et al. 2003, AJ, in press (astro-ph/0301135)
9. Bromm, V., Coppi, P. S., & Larson, R. B. 1999, ApJ, 527, L5
10. Bromm, V., Coppi, P. S., & Larson, R. B. 2002, ApJ, 564, 23
11. Nakamura, F., & Umemura, M. 2001, ApJ, 548, 19

⁴ See <http://lisa.jpl.nasa.gov/>

12. Abel, T., Bryan, G. L., & Norman, M. L. 2002, *Science*, 295, 93
13. Pudritz, R. E. 2002, *Science*, 295, 68
14. Larson, R. B. 2002, *MNRAS*, 332, 155
15. Kroupa, P. 2002, *Science*, 295, 82
16. Rees, M. J. 1976, *MNRAS*, 176, 483
17. Bate, M. R., Bonnell, I. A., & Bromm, V. 2002, *MNRAS*, 332, L65
18. Bate, M. R., Bonnell, I. A., & Bromm, V. 2003, *MNRAS*, in press (astro-ph/0212380)
19. Bromm, V., & Loeb, A. 2003, *ApJ*, submitted (astro-ph/0212400)
20. Bromm, V., Kudritzki, R. P., & Loeb, A. 2001, *ApJ*, 552, 464
21. Christlieb, N., et al. 2002, *Nature*, 419, 904
22. Mackey, J., Bromm, V., & Hernquist, L. 2003, *ApJ*, in press (astro-ph/0208447)
23. Omukai, K., & Nishi, R. 1998, *ApJ*, 508, 141
24. Omukai, K., & Palla, F. 2001, *ApJ*, 561, L55
25. Ripamonti, E., Haardt, F., Ferrara, A., & Colpi, M. 2002, *MNRAS*, 334, 401
26. Tan, J. C., & McKee, C. F. 2003, these proceedings
27. Palla, F., Salpeter, E. E., & Stahler, S. W. 1983, *ApJ*, 271, 632
28. Omukai, K., & Inutsuka, S. 2002, *MNRAS*, 332, 59
29. Wolfire, M. G., & Cassinelli, J. P. 1987, *ApJ*, 319, 850
30. Madau, P., Ferrara, A., & Rees, M. J. 2001, *ApJ*, 555, 92
31. Mori, M., Ferrara, A., & Madau, P. 2002, *ApJ*, 571, 40
32. Thacker, R.J., Scannapieco, E., & Davis, M. 2002, *ApJ*, 581, 836
33. Loeb, A., & Haiman, Z. 1997, *ApJ*, 490, 571
34. Todini, P., & Ferrara, A. 2001, *MNRAS*, 325, 726
35. Machacek, M. E., Bryan, G. L., & Abel, T. 2001, *ApJ*, 548, 509
36. Machacek, M. E., Bryan, G. L., & Abel, T. 2003, *MNRAS*, 338, 27
37. Omukai, K. 2000, *ApJ*, 534, 809
38. Bromm, V., Ferrara, A., Coppi, P. S., & Larson, R. B. 2001, *MNRAS*, 328, 969
39. Schneider, R., Ferrara, A., Natarajan, P., & Omukai, K. 2002, *ApJ*, 571, 30
40. Lamb, D. Q., & Reichart, D. E. 2000, *ApJ*, 536, 1
41. Ciardi, B., & Loeb, A. 2000, *ApJ*, 540, 687
42. Bloom, J. S., Kulkarni, S. R., & Djorgovski, S. G. 2002, *AJ*, 123, 1111
43. Kulkarni, S. R., et al. 2000, *Proc. SPIE*, 4005, 9
44. Totani, T. 1997, *ApJ*, 486, L71
45. Wijers, R. A. M. J., Bloom, J. S., Bagla, J. S., & Natarajan, P. 1998, *MNRAS*, 294, L13
46. Blain, A. W., & Natarajan, P. 2000, *MNRAS*, 312, L35
47. Bromm, V., & Loeb, A. 2002, *ApJ*, 575, 111
48. Heger, A., Fryer, C. L., Woosley, S. E., Langer, N., & Hartmann, D. H. 2003, *ApJ*, submitted (astro-ph/0212469)
49. Barkana, R., & Loeb, A. 2003, *Nature*, in press (astro-ph/0209515)
50. Miralda-Escudé, J. 1998, *ApJ*, 501, 15
51. Rees, M. J. 1984, *ARA&A*, 22, 471
52. Becker, R. H., et al. 2001, *AJ*, 122, 2850
53. Djorgovski, S.G., Castro, S., Stern, D., & Mahabal, A. A. 2001, *ApJ*, 560, L5
54. Fan, X., Narayanan, V. K., Strauss, M. A., White, R. L., Becker, R. H., Pentericci, L., & Rix, H.-W. 2002, *AJ*, 123, 1247
55. Loeb, A., & Peebles, P. J. E. 2002, *ApJ*, submitted (astro-ph/0211465)
56. Loeb, A., & Rasio, F. A. 1994, *ApJ*, 432, 52
57. Oh, S.P., & Haiman, Z. 2002, *ApJ*, 569, 558
58. Haiman, Z., Rees, M. J., & Loeb, A. 1997, *ApJ*, 476, 458; erratum 484, 985
59. Wyithe, J. S. B., & Loeb, A. 2003b, *ApJ*, submitted (astro-ph/0211556)
60. Baumgarte, T. W., & Shapiro, S. L. 1999, *ApJ*, 526, 941